Chapter

Development of a Novel Electromagnetic Rewarming Technology for the Cryopreservation of Stem Cells with Large Volume

Shen Ren, Zhiquan Shu, Jiaji Pan, Ji Peng, Junlan Wang, Chunhua Zhao and Dayong Gao

Abstract

Applications of stem cells have been playing significant roles in scientific and clinical settings in the last few decades. The foundation of these approaches is successful cryopreservation of stem cells for future use. However, so far we can only cryopreserve stem cell suspension of small volumes in the order of 1 mL mostly due to the lack of an effective rewarming technique. Rapid and uniform rewarming has been approved to be beneficial, and sometimes, indispensable for the survival of cryopreserved stem cells, inhibiting ice recrystallization or devitrification. Unfortunately, the conventional water bath thawing method failed in providing the rapid and uniform rewarming. The conversion of electromagnetic (EM) energy into heat provides a possible solution to this problem. This chapter will focus on (1) analysis of the combined EM and heat transfer phenomenon in the rewarming of a biospecimen, (2) numerical investigation of the rewarming system, (3) practical setup of an EM resonance system, and (4) test of heating performance with large volume of cells.

Keywords: stem cell, cryopreservation, large samples, electromagnetic, rapid-uniform rewarming

1. Introduction

Cryopreservation is one the most essential techniques that has been widely used for preserving stem cells in scientific research and cellular therapies [1]. The principle of cryopreservation is to use the super low temperature to reduce the biological and chemical reactions in living stem cells. The expansion in clinical tests for biomedical applications revealed the limitations of the current preservation technologies, i.e., only the small volumes of stem cells can be successfully cryopreserved. In the case of large samples such as bulk volume of cells, tissues, or organs,

cryopreservation often fails because of the damage caused by ice crystal growth and thermal stress within the bio-samples [2, 3].

In 1960s, Mazur proposed "two-factor hypothesis" of freezing injury based on the study of Chinese hamster tissue [4]. During the cooling process, two distinct types of cryoinjuries determine the life or death of the cells, which are affected by the cooling rate. Neither too high nor too low the cooling rate is favored for the cryopreservation (**Figure 1**).

When cells are cooled down to subzero temperatures under a normal pressure, ice crystals emerge and grow in the suspensions outside the cell membrane in the beginning [5]. The external ice growth into cells is blocked by the plasma membrane. The cytoplasmic region remains unfrozen and in the supercooled state [6]. However, the increase of osmolality and chemical potential difference across cell membranes due to the external ice formation will serve as a driving force for mass transfer between the intracellular components and extracellular environment, pulling water out of cells. If the cooling is too rapid, there is insufficient time for the water to flow out of the cells. As the temperature goes down rapidly, the unfrozen and supercooled state is disturbed and the intracellular ice formation (IIF) happens [7]. The lethal IIF can rupture the cell membranes and lead to the cell death. On the other hand, if the cooling rate is too slow, intracellular ice may be reduced or avoided. The plenty of time permits water transport out of the membrane under the influence of the osmolality difference. Cells then suffer from high concentration of intracellular solute/electrolytes (so called "solution effects") and severe dehydration. The slower cooling process may expose the cells to "solution effects" for a longer time, which is unacceptable for the cells. Therefore, the cooling rate may not be too high or too low based on the "two-factor hypothesis".

Later in 1984, Mazur reported the rapid rewarming can 'rescue' the rapidly frozen cells [6]. Though the fast cooling process produces intracellular ice, the crystals tend to be small. Due to the unstable thermal properties, during rewarming, small crystals formed at lower temperature aggregate to become larger crystals. The process referred to as recrystallization. It has been proved that the cells cooled at rate far beyond the optimal one will survive if warmed at very rapid rate, but cells do not survive if warmed slowly [8, 9]. Besides the rapid rewarming rate, uniformity of temperature distribution also plays an important role to the survival of the samples [10]. Thermal stress caused by the temperature gradients will lead to the crack of the brittle material, especially the larger systems [11]. Thus, both of fast and homogeneity are essential in the thawing. A rapid-uniform

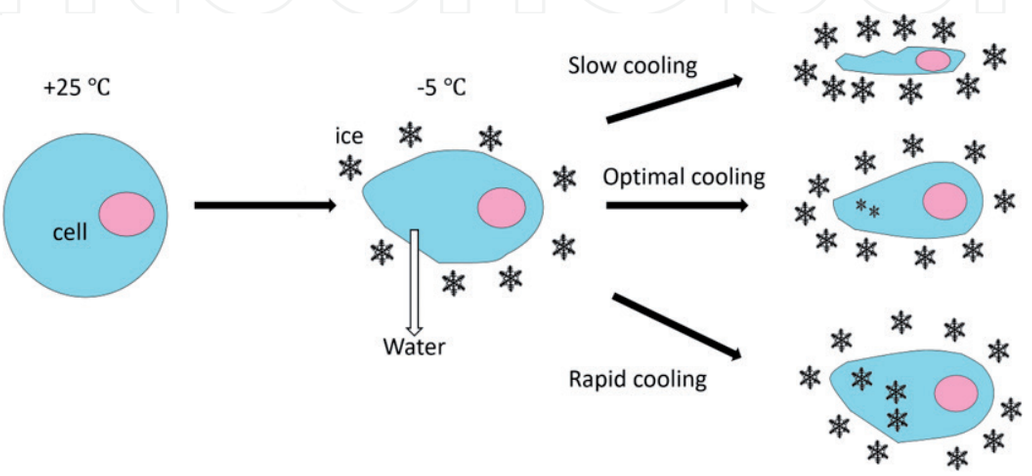

Figure 1.
Schematic drawing of physical events in cells during freezing.

rewarming technology is needed to successful cryopreservation of stem cells with large volume.

A typical cryopreservation procedure is composed of five steps:

1. addition of appropriate cryoprotective agents (CPAs),

2. cooling at an optimal rate,

3. storage at the low temperature (e.g. -80°C freezer or – 196°C liquid nitrogen tank),

4. rearming to physiological temperature, and

5. removal of the CPAs.

Over the past decades, scientists made significant progress in the methods and protocols of addition/removal of CPAs, approaches of cooling to the target temperature, and strategies to preserve biomaterials at sub-zero temperature environment. However, in the scientific and clinical applications, convective rewarming of the cryopreserved samples, typically thawing in a 37°C water bath, remains the gold standard for small samples [12].

2. Rewarming concerns

Warming in the water bath is a convective rewarming approach in which heat is transferred from the outer boundaries to the inner portion of the cryopreserved biological samples. Because of the high specific heat of biological materials, it requires a great amount of heat to rewarm them. Another obstacle for the rewarming process is the low thermal conductivity of biomaterials. Heat cannot be quickly transmitted into the core area of large samples. For a small volume of cell suspensions, the problem caused by the lower thermal conductivity may possibly be solved by the design of sample holder (e.g. maximize the sample holder's ratio of surface area to volume) [13]. However, for larger system with much smaller ratio of the surface area to the volume, they cannot be sliced or pressed into a thin film to increase the heat transfer area for convective warming in water bath. In this case, a large temperature difference will occur and lead to thermal stresses that can result in fracture of the samples during rewarming. Therefore, the traditional method of convective rewarming at the sample surface is not appropriate for the cryopreservation of large volume of biomaterials. A uniform and rapid rewarming method is needed to meet the urgent needs in tissue engineering and cellular therapy, which may be achieved by a volumetric rewarming technique, e.g., electromagnetic heating.

3. Electromagnetic rewarming

3.1 Fundamentals of electromagnetics

The electromagnetic field is a combination of the electric field and the magnetic field generated by electrically charged objects. The electric field and magnetic field are coupled with each other. A time varying electric field (contrary to static field) induces magnetic field changing over time, and vice versa. The distribution and

propagation of electromagnetic fields are governed by Maxwell's equations. An electromagnetic wave is the propagation of the electromagnetic field through media such as air, water, etc., or in vacuum. This propagation also refers to radiation transmitting the electromagnetic energy, momentum and angular momentum through space. As one of the basic forces in nature, the propagating electromagnetic fields interact with other materials and generate different effects depending on the frequency and power. Based on the mechanisms behind these interactions between electromagnetic waves and other materials, electromagnetic waves have been applied in numerous aspects including: telecommunications such as mobile phone calling, the short wave broadcast, TV signal transmission and connection between the spaceship and the base on earth, remote sensing for the weather forecasting, land mapping, infrared radiation detecting, X-rays and computer tomography (CT) or the disease diagnoses, and radiotherapy which employs higher energy radiation to kill cancer cells. These various applications are closely related to the spectrum of electromagnetic waves. The most commonly used frequency band is at radio frequency (RF) electromagnetic wave and microwave.

3.2 Electromagnetic rewarming

The thermal effects of electromagnetic waves benefit the organism on earth even long before the prehistory. The thermal energy transmitted by the electromagnetic waves emitted from the sun allows the survival of plants, animals. This electromagnetic wave emitted from the sun, or sunlight, is distributed across almost the entire spectrum but with major intensity on infrared, visible, and ultraviolet frequency ranges. These major components visible light has a frequency range in several hundreds of THz. Higher frequency electromagnetic waves such as X-rays carry much higher energy and are used for radiation therapy killing the tumor cells by ionizing the molecules. In the lower frequency range, electromagnetic waves (radio frequency electromagnetic waves, microwave) with less energy can hardly excite ionization, but can result in thermal effects with materials.

The investigation of the heating phenomenon by microwave occurred in the 1940s. A candy bar under an active microwave generating devices melted and the engineer used this observation to develop equipment for preparing and heating food utilizing the thermal effects of microwave radiation. Since then, not only has the commercialization of the microwave oven become widespread, scientists also began to study the potential benefits for industry and medicine. Most of food is a dielectric material that can interact with the electromagnetic fields in the microwave oven due to a large portion of water in the contents. The water molecules are dipole molecules comprising an electrical positive charged end and an electrical negative charged end. Under the influence of electric fields, these dipole molecules will align themselves with the applied electric fields. When the directions of external electric fields are changing as in the oscillating electromagnetic waves, the dipole molecules will rotate to follow up with the changing fields. The interactions between the rapid changing electromagnetic fields and water dipole molecules will cause mechanical friction forces among the water molecules. The frictions between these micro molecules generate heat volumetrically. Similarly, to the food in the microwave oven for heating, the biological materials in cryopreservation are organisms that are primarily composed of water. Therefore, microwave can also be used for the heating of cryopreserved biological systems.

When using microwave as the rewarming approach in the cryopreservation, the biomaterials interact with the applied electromagnetic field. Since most biomaterials are nonmagnetic, the forced movement of molecules is mainly due to the electric field component of the electromagnetic field. As shown in **Figure 2**, a distinct

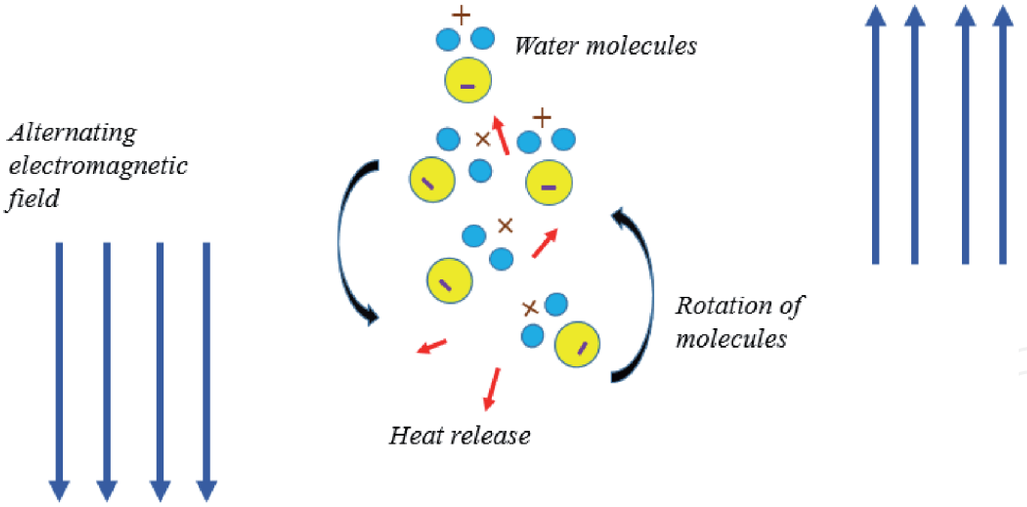

Figure 2.
Illustration of heat generation under the influence of electromagnetic waves.

advantage of microwave rewarming compared with the traditional water bath rewarming is that the heat is generated over the entire region of the material which can lead to volumetric and uniform heating.

The electrical parameter that characterizes the interaction between the material and electric field component is the relative complex permittivity, or dielectric property, expressed in Eq. (1):

$$\varepsilon_r = \varepsilon' - i\varepsilon'' \ . \tag{1}$$

The real part of complex permittivity, ε', also known as dielectric constant, represents the ability of storing electric field energy. The imaginary part of complex permittivity, ε'', known as dielectric loss, represents the ability to absorb electric field energy. The heat generation density q due to the electromagnetic rewarming in the material is given by Eq. (2):

$$q = \pi f \varepsilon_0 \varepsilon'' |E|^2 , \tag{2}$$

where f is the frequency of electromagnetic wave, ε_0 is the electric permittivity of free space, $|E|$ is the root mean square magnitude of the electric field. To deal with the slow warming obstacle due to the high heat capacity, two straightforward solutions can be figured out based on the heat generation principle. One is to select material with higher dielectric loss, and the other approach is to increase the magnitude of the electric field applied to the cryopreserved biomaterial. Provided a strong electric field intensity, the rewarming of cryopreserved biomaterials by electromagnetic wave could be ultrafast which seems to be a promising approach to avoid recrystallization and/or devitrification.

3.3 Previous electromagnetic rewarming attempts by Cryobiologists

The development of electromagnetic rewarming systems is limited by the cost and inadequate theoretical guidance. The establishment of an electromagnetic resonance rewarming system involves the selection of frequency source and power, manufacturing of the resonance chamber, optimization of the electromagnetic energy feeding approach to the cryopreserved materials. Setting up a specific resonance rewarming system can take a few months to years and requires substantial

funding support. When the system is going to be scaled up to materials of a larger dimension, various parameters of the system should be replaced which will extend the time required for the optimization. The first experimental investigation of using electromagnetic energy in cryopreservation began in the 1970s. In Kettrer's experiment [14], 20 kidneys rewarmed by a microwave generation device with power control were considered partial success. By using a commercial 1.35 kW Toshiba microwave oven which generated by 2.45 GHz magnetron, Guttman [15] reported the electromagnetic rewarming of 16 cryopreserved canine kidneys. Half of the dogs receiving transplantation of these kidneys survived months.

However, in Pegg's attempt [16] to repeat the rewarming of dog kidneys with commercial microwave oven, none of the post-thawing dog kidneys function properly.

Another device designed by Burdette [17] generated an electromagnetic field with an open electromagnetic illumination system. The frequency can be adjusted to several distinct values. The rewarming results of rabbit and canine kidneys were published without the following viability analysis.

These preceding explorations opened a new avenue for cryobiologists, most specialized in biomechanical and biochemical physics, to implement new technologies from electrical engineering in the application of cryopreservation. A major problem for these early investigations of electromagnetic rewarming is that the frequency of the commercial microwave oven is too high to penetrate into the inner part of the cryopreserved biomaterials. A good uniformity should be achieved with lower frequency electromagnetic waves. In addition, electromagnetic rewarming can result in a 'thermal runaway' problem because the dielectric loss of biomaterials generally increases with temperature during rewarming process, which leads to an increasing temperature difference across the sample volume.

Thermal runaway phenomenon is depicted in **Figure 3**. Due to the complex interactions between the material and the applied electromagnetic wave, and nonuniformity of material properties, the temperature distribution may not be that uniform initially. The slightly warmer area of the biological samples has a higher ability to absorb energy from electromagnetic waves and convert into heat than colder area. The temperature difference between these components will be magnified. When the difference in governing properties is significant and favors the ultrafast thawing of the hot area, the nonuniform temperature gradient is even intensified.

To avoid the localized warming associated with 'thermal runaway' and limited penetration depth for the 2.45 GHz high frequency electromagnetic waves, more delicate controlled electromagnetic rewarming systems operating in lower frequencies are required for cryopreservation. Thereafter, a rewarming system using helical coil to generate tens of MHz electromagnetic waves was used to rewarm CPA solutions as a preliminary trial [18]. But the rewarming rate was moderate achieved by this open system. Later on, a few scientists reconsidered the electromagnetic

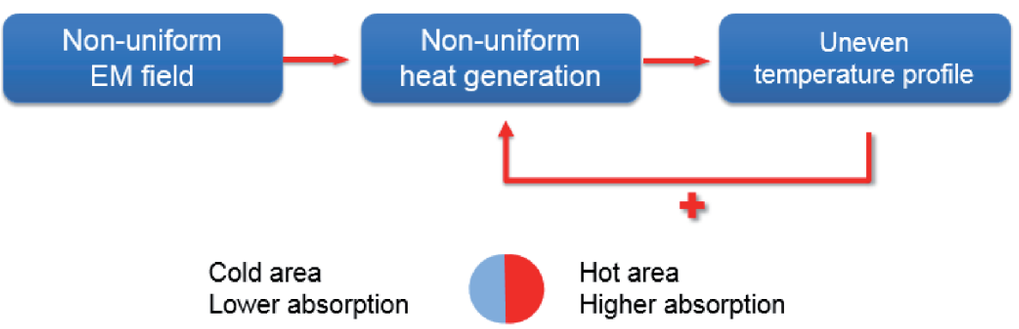

Figure 3.
Introduction of the 'thermal runaway' phenomena: The appearing of large temperature gradient by electromagnetic rewarming.

rewarming in closed systems to confine electromagnetic energies [19, 20]. Unlike the commercial microwave oven in which the generated signal shifted around ±50 MHz, the electromagnetic wave was synthesized by voltage-controlled oscillators. The stability of frequency was improved so that the design of chamber could fit with the electromagnetic source and establish resonant state to concentrate the electromagnetic energy.

A major problem for these resonant systems may come from an intention to reduce the non-uniformity by adopting multimode resonant cavities. In Rachman's electromagnetic resonance cavity rewarming system [19], two resonant states of the cavity were excited (TE111 and TM010). Another multimode cavity rewarming system designed by Robinson [20] excited three different modes. The results of the warming test for CPA solutions were improved while the spatial temperature difference was not greatly reduced, which means thermal runaway could not be eliminated. The reason behind this is due to the interaction between the cryopreserved CPAs and the properties of the resonant cavity. Multimode cavities resonating at different frequencies bring more difficulties in the control of signal frequency at each port to feed electromagnetic energy into the cavity. Hence, a single mode resonant cavity which excites only at a specific frequency may be superior in the control of field distribution in the rewarming process.

Our goal is to achieve effective cryopreservation protocol for bulk volume of stem cells. In this chapter, the target is to improve electromagnetic rewarming systems for the rapid-uniform rewarming, laying down the foundation for the cryopreservation of biomaterials with large volume.

4. Characterization of essential physical properties of CPA solutions

4.1 Determination of the electrical properties

The dielectric properties of the biomaterials characterize the interaction between applied electromagnetic field and the biomaterials, and thereby determine the absorption of electromagnetic energy by the biomaterials [21, 22]. The dielectric properties are temperature dependent. If the warmer part of the biomaterial absorbs more heat, the temperature at that warmer part would be further increased, increasing temperature gradients, and therefore inducing thermal stresses. A large thermal stress can destroy the viability of cryopreserved materials and can be even more threatening to bulky systems [23, 24]. Since the dielectric properties play a key role in the absorption of electromagnetic energy, it is a priority to discover the dielectric properties of the biomaterials. In cryopreservation, particularly in vitrification using a high concentration cryoprotective agent, the CPA/vitrification solutions dominate the properties of the cell suspensions or tissues. Hence, the dielectric properties of the CPA/vitrification solutions should be determined so that electromagnetic rewarming can be optimized.

The measurement of the dielectric properties of biomaterials requires sensing and monitoring tools. In many biomedical applications, various measurement methods including transmission and reflection techniques have been used to determine dielectric properties [25–29].

The samples measured by transmission and reflection methods usually are fixed without morphologically change. But in the application of electromagnetic rewarming, the measurement of dielectric properties must be carried out in the subzero temperature range which may involves phase change and rules out the possibility using transmission and reflection techniques. The cavity perturbation method has been used for measuring the electric properties of different kinds of

materials [30–33] due to its ability to measure the dielectric properties of low loss dielectric materials [34]. In the subzero temperature range, the dielectric properties of biomaterials and CPA/vitrification solutions can be very small. Therefore, in this work, we adopted a cavity perturbation method to determine the dielectric properties of three different vitrification solutions at low temperatures. Briefly, a resonant cavity was designed and manufactured to measure the dielectric properties of cryopreserved biomaterials at 434 MHz. By inserting samples with different permittivity into the resonant cavity, the resonant frequency and quality factor could be changed. From the variation of the resonant frequency and the quality factor, the dielectric properties can be derived.

4.1.1 Perturbation theory

Through the change of resonant frequency Δf and inverse of quality factor ΔQ, the dielectric property (or complex permittivity) of CPA/vitrification solutions was obtained. The mathematical derivation is shown by following Equations [35, 36]:

$$\frac{\Delta\tilde{\omega}}{\tilde{\omega}} = \frac{\Delta f}{f_0} + \frac{i}{2}\left(\frac{1}{Q} - \frac{1}{Q_0}\right) \tag{3}$$

$$\frac{\Delta\tilde{\omega}}{\tilde{\omega}} = \frac{\int_{V_s}\left(\Delta\varepsilon EE_0^* + \Delta\mu HH_0^*\right)dv}{\int_{V_c}\left(\varepsilon EE_0^* + \mu HH_0^*\right)dv} \tag{4}$$

where Δf and ΔQ are resonant frequency and quality factor of unperturbed cavity, $\boldsymbol{E_0}$ and $\boldsymbol{H_0}$ represent electric field and magnetic field inside the unperturbed cavity, $\boldsymbol{E}$ and $\boldsymbol{H}$ represent those fields for the cavity with sample to be measured inside, ε and μ are complex permittivity and permeability of the sample, i is an imaginary number of which the square equals -1. More simplification can be applied to Eq. (4), equating the real and imaginary parts and the following relationship will be obtained:

$$\Delta f = k_1 \frac{\varepsilon' - 1}{\varepsilon' + 2} \tag{5}$$

$$\Delta\left(\frac{1}{Q}\right) = k_2 \frac{\varepsilon''}{\left(\varepsilon' + 2\right)^2} \tag{6}$$

k_1 and k_2 are constants to be determined.

4.1.2 Dielectric property measurement system

The experimental system is shown in **Figure 4**. A rectangular single-mode resonant cavity resonating at around 434 MHz was manufactured. The dimension of the cavity was designed to 680 × 400 × 350 mm. Copper plates were used to manufacture the cavity due to its high conductivity (to prevent electromagnetic leakage).

4.1.3 Calibration of the measurement system

Water, methanol, ethanol, 1-propanol, 2-propanol, ethylene glycol and cyclohexane samples with known properties were used for calibration of the cavity to determine k_1 and k_2. The properties of these calibration solutions were reported by Robinson [37].

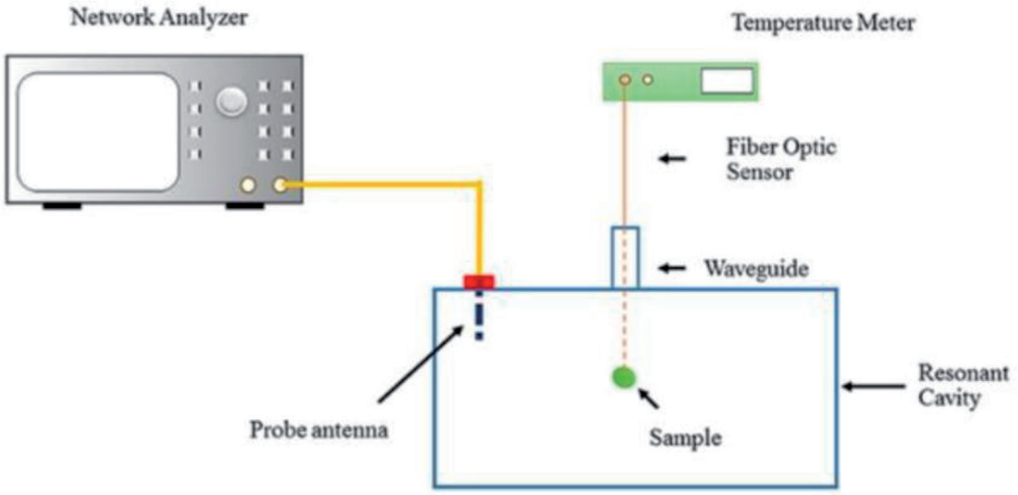

Figure 4.
Schematic of the system for measurement of dielectric properties.

Once k_1 and k_2 had been obtained, unknown cryopreserved biomaterials can be measured by the system. Similarly, the resonant frequency and quality factor were changed. According to the shift frequency and quality factor of the cavity, complex permittivity of samples can be derived.

4.2 Determination of the thermal properties

4.2.1 Measurement of specific heat

To determine the temperature-dependent specific heat capacity, Differential Scanning Calorimetry (DSC) was used to take accurate measurement of various sample solutions. Isothermal step scan method is adopted to minimize the experimental error. The latent heat was incorporated into the effective specific heat capacity when the phase transition occurs.

4.2.2 Measurement of thermal conductivity

Thermal conductivity of sample solutions was measured using a micro thermal sensor developed by Liang, et al. [38] and manufactured in the lab. The sensor works on the principle of Transient Hot Wire (THW). This miniaturized device utilizes a SiO2/Au/SiO2 sandwiched structure to protect the microfabricated serpentine gold coil, which functions as both the heater and a passive thermometer. The sensor has already been tested and shown to measure thermal conductivity of biomaterials and solutions with high accuracy, repeatability and system reliability.

5. Theoretic analysis and numerical simulation to improve the electromagnetic resonance system

5.1 Introduction

Previous cryobiologists have developed electromagnetic cavity rewarming for large biomaterials. Evans [39], Robinson [37] and Luo [40] built electromagnetic heating systems that could resonate at around 434 MHz but working at different modes. The sample was placed at the center with a large magnitude of the electric

field, which is critical to rapid rewarming. The size of the sample was controlled to reduce temperature gradients resulted from the electromagnetic field attenuated away from the center. For multimode resonant cavity rewarming system, it could be difficult to control the resonant state or field distribution with several EM power inputs. While single mode cavity system is easier to concentrate a strong EM field and control in the rewarming process. Therefore, multimode resonant rewarming systems are excluded for optimization here. According to the warming results, electromagnetic rewarming has already demonstrated more effective than traditional water bath method. However, further improvement of the electromagnetic rewarming system is still needed to optimize the rewarming protocol of bulk volume of cells.

Multiple theoretical analysis and numerical simulations had been accomplished [41–43] on different design possibilities of electromagnetic rewarming systems. Method of moments (MoM) was implemented to calculate and analyze the electric filed intensity and profile [42] and the method of finite-difference time-domain (FDTD) was applied to investigate the post-thawed temperature profile [44]. Another attempt involving the resonance rewarming in the numerical model combined with nanoparticles to improve the warming rate. However, in this study, the model was based on the power consumption at 8000 W [45] that is hard to achieve in the real-world.

In this section, a more efficient and effective model based on finite element method combining electromagnetic wave propagation and heat transfer process was presented. The optimization of the shape of cryopreserved sample was performed numerically. The essential physical properties of several sample solutions including complex permittivity, specific heat, and thermal conductivity characterized experimentally in the previous studies were used in this simulation test.

5.2 Theoretical formulations

The electromagnetic resonant system setup showed in **Figure 5** consists of a signal generator with voltage control at lower scale, a power oscillator, a resonant cavity, a coaxial transmission wire, and a temperature sensor. An antenna made of high electrical conductivity material was used to excite the electric field and create a standing wave pattern of electromagnetic field inside the rewarming cavity. A sample holder contained cryopreserved stem cells or other biomaterials was place in the center of the cavity, where the strongest electric field was established to achieve the fast rewarming.

Most of the cryopreserved biomaterials are insensitive to the magnetic field, e.g. the stem cells, with electrical parameters including, ε (absolute permittivity, $F \cdot m^{-1}$), σ (conductivity, $S \cdot m^{-1}$), and $\mu = \mu_0$ (magnetic permeability of the free space, $H \cdot m^{-1}$,), the frequency domain Maxwell equations were used to calculate the electric field profile in the cryopreserved material:

$$\nabla \times E = -j\omega\mu H - M \tag{7}$$

$$\nabla \times \nabla \times H = -j\omega\varepsilon E + \sigma E + J \tag{8}$$

where E is the electric field intensity ($V \cdot m^{-1}$), and H is the magnetic field intensity ($A \cdot m^{-1}$). Here, M is the magnetization filed intensity ($A \cdot m^{-1}$) that equivalent to the H term, and J is the flowing current density ($A \cdot m^{-2}$) that equivalent to the E term. Both M and J can be ignored since none of magnetic and

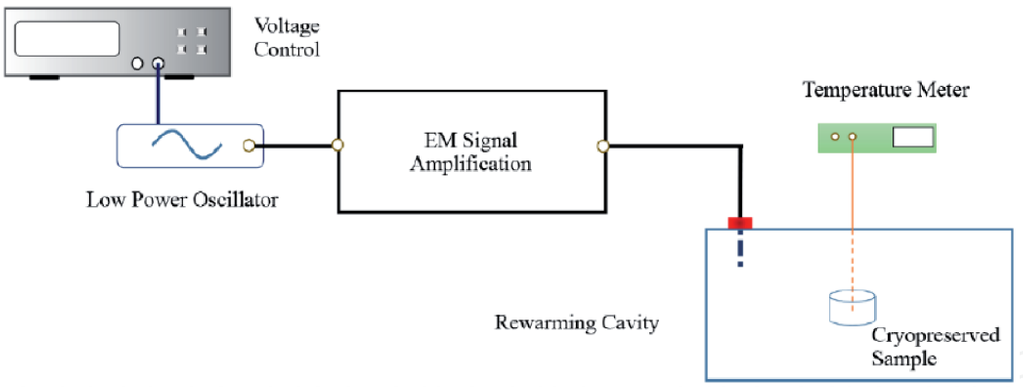

Figure 5.
Schematic description of the experimental setup of the EM rewarming system.

electric source was established inside of the given geometry. ω is the angular frequency of the EM field ($rad \cdot s^{-1}$). The absolute permittivity $\varepsilon = \varepsilon' - i\varepsilon''$, where ε' is the real part, stands for the dielectric constant that describe the space's ability to hold the electric power within the control volume. ε'' is the imaginary part, stands for the dielectric loss that describe the space's ability to harness electric power. Heating is generated through the vibration of dipolar molecules affected by the electric field. The term q represents the absorbed electric power in the material is described as:

$$\nabla \times E = -j\omega\mu H - M \tag{9}$$

$$q = \pi f \varepsilon_0 \varepsilon'' |E|^2 \tag{10}$$

where f (Hz) denotes the frequency of the electromagnetic field. q ($W \cdot m^{-3}$), the total absorbed power from the electromagnetic field, can be combined into the heat transfer equation as the heat source term [46]:

$$\rho C \frac{\partial T}{\partial t} = \nabla \cdot (k \nabla T) + \pi f \varepsilon_0 \varepsilon'' |E|^2 \tag{11}$$

where $\rho\left(kg \cdot m^{-3}\right)$ represents the density of the cryopreserved material, C $\left(\mathrm{J} \cdot kg^{-1} \cdot K^{-1}\right)$ denotes the specific heat, k ($W / m \cdot K$) is the thermal conductivity, T (K) is the temperature of the cryopreserved material, and t (s) is the time in the heating process.

In this numerical modeling analysis, the thermal properties of the cryopreserved material were preset to be temperature-dependent. The specific heat and thermal conductivity at different temperatures were captured once the temperature profile in the Eq. (11) was determined. With the updated thermal and electrical properties over the interested temperature range, the electromagnetic field profile was calculated. Cryopreserved material's dielectric loss ε'' and applied electric filed intensity changed the heating source. Thus, the temperature and electric fields are coupled. Adiabatic ($q_{conv} = 0$) assumptions were applied to the boundary conditions to eliminate the natural convection within the cavity. The perfect conductor assumption was also applied to the inner surface of the resonant cavity ($\vec{n} \times E = 0, \vec{n}$ denotes the inner wall's unit vector of the cavity).

5.3 Numerical simulation

The numerical modeling was setup with COMSOL Multiphysics (COMSOL, Burlington, MA, USA), applying the finite element method. Adopting the analytical process discussed in the theoretical formulation section, the thermal science and combined electromagnetic rewarming system in the resonant chamber as shown in **Figure 6**. In this numerical investigation, the thermal and electrical parameters of the model were determined follow the methods discussed in the previous section.

Nyquist criterion was applied to the meshing grid of the simulation. The maximum size of the element grid was contained smaller than half of the wavelength of the electromagnetic wave. Six grids per wavelength in the finite element analysis was also employed to solve the Maxwell's equation [47].

Tetrahedral grids were selected in this study due to smaller grid size comparing to the discretization of the resonant rewarming system. Once the tetrahedron grid applied, the grid size of the resonant chamber was calculated to be less than 10% of the wavelength of electromagnetic wave. In the mesh preparation (shown in **Figure 7**), different meshing approaches were adopted for different components of the system. Refined meshes were created near the boundaries of surfaces (in total, about 988,000 elements were generated). The area around probe antenna

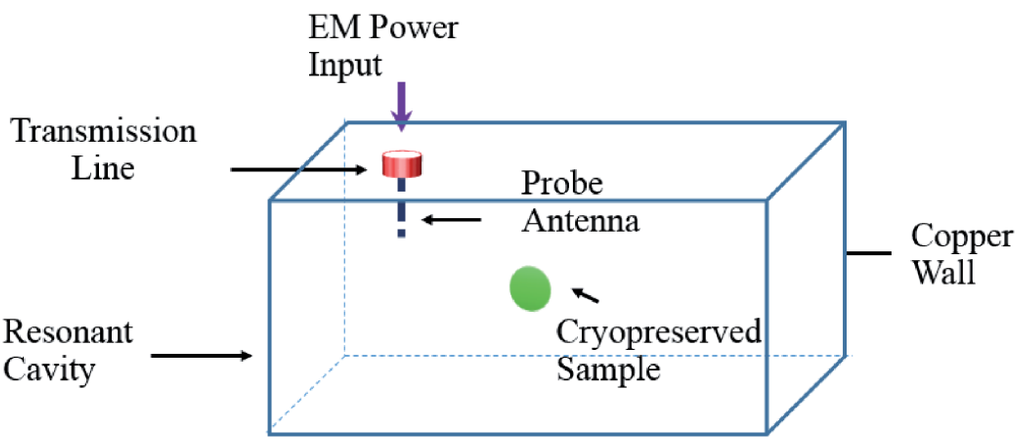

Figure 6.
Schematic description of the simulated resonant EM rewarming cavity.

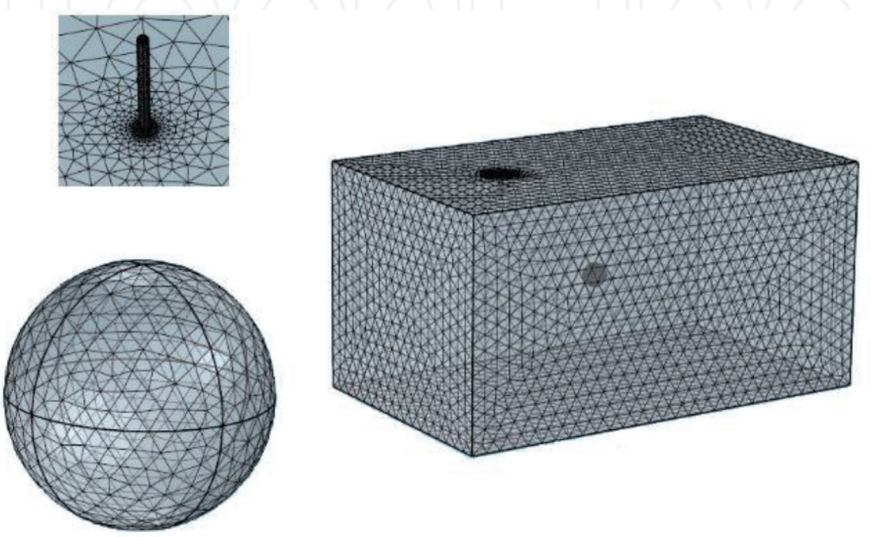

Figure 7.
Geometric gridded model of the resonant cavity for simulation.

and central part of the sample holder were treated with the enhanced meshing. A smaller grid size (about 163,000 elements) will diminish the difference of the temperature profile less than 0.5% over the entire field.

5.4 Results

5.4.1 Field distributions in the resonant cavity

The prepared simulation model was validated with the analytical results. In the model, the resonant frequency of the chamber was 434.767 MHz, consistent with the frequency from the analytical result. When the chamber was at the resonant state, the normalized electric field intensity profile was plotted for both of the simulated result and analytic result in the resonant cavity was plot in comparison with the analytic solution (**Figure 8**), which proofed a good alignment between two results. As the position advancing to the central part of the cavity, the intensity of the electric field increased significantly. Hence, the cryopreserved bio-sample was designed to be placed in the central to achieve a fast rewarming process by absorb more electromagnetic power.

5.4.2 Various sample holder shape's effect on the rewarming process

The effect of sample holder's shape to the rewarming was studied to minimize the injury to the biomaterials caused by non-uniform thawing. On the other side, different sample holders might be selected based on the size and structure of the biomaterials. Considering the hardness to accurate calculate the energy conversion between the cavity and the sample through analytical solution, and precise temperature profile monitoring over the entire sample space through experiment, in this simulation, a total of four different sample holder shapes (geometry details shown in **Table 1**) with the same sample volume of 25 mL were calculated to study the difference over the rewarming process. The heating started at the initial temperature set to −80° C and ended at 0°C. The average rewarming rates of cylindrical, ellipsoidal, spherical, and cubic holders were 72.1, 63.5, 46.1, and 22.8° C/min, respectively. From the fast rewarming perspective, cylindrical and ellipsoidal shapes were the top choices.

Later, the temperature profile at the end of the rewarming was investigated. As shown in **Figure 9**, the temperature gradients that defined as the temperature

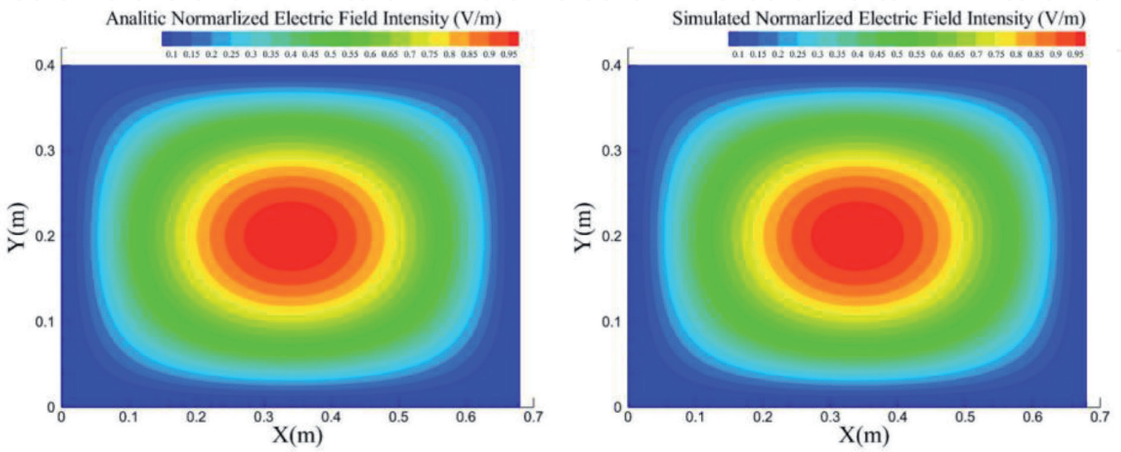

Figure 8.
Distribution of the electrical field magnitude at the central cross-sectional plane in the electromagnetic rewarming chamber. Analytical and simulated results show that electric field energy is focused in the center of the cavity.

Parameter	Value (mm)
Radius of sphere	18
Radius of cylinder	18
Height of cylinder	20
a-Semi axis of ellipsoid	23
b-Semi axis of ellipsoid	14
c-Semi axis of ellipsoid	18
Side length of cube	29

Table 1.
Dimensions of sample holder shapes.

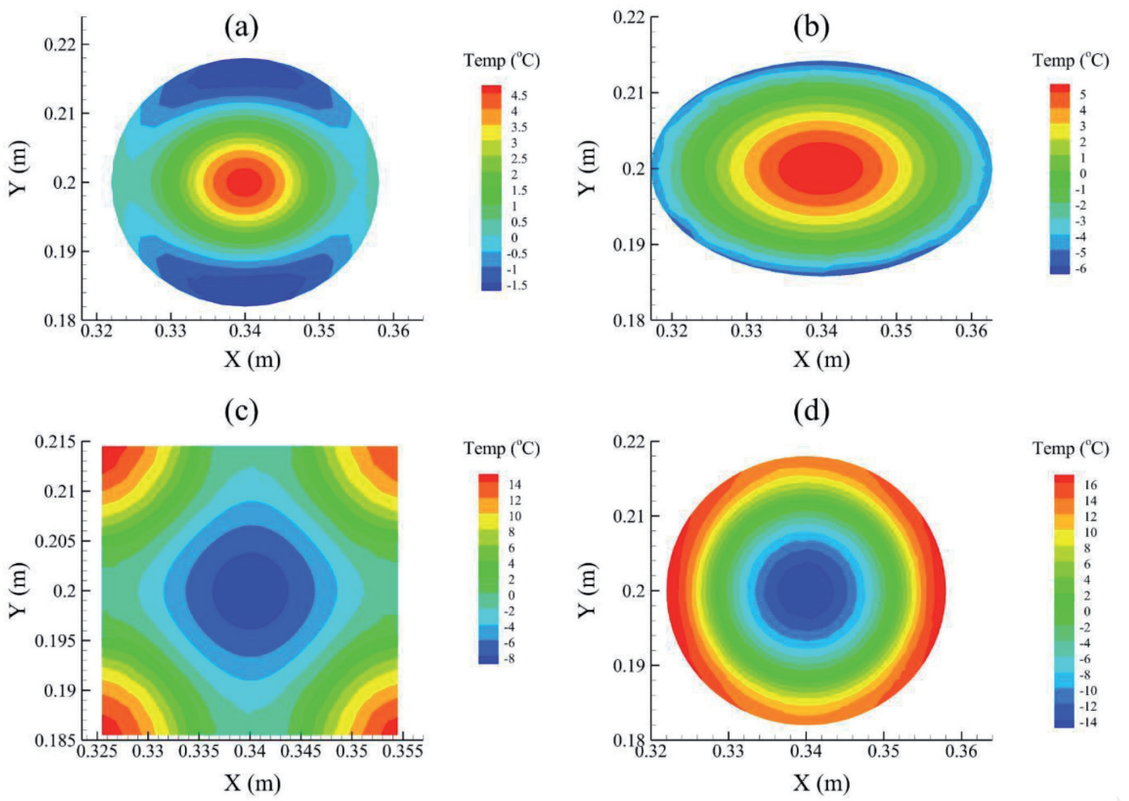

Figure 9.
Simulated post thawing temperature distribution of cryopreserved sample solution in different sample holder shapes. (a) Spherical shape; (b) ellipsoidal shape; (c) cubic shape; (d) cylindrical shape. The spherical and ellipsoidal samples manifested more uniform temperature distribution than cubic and cylindrical samples.

difference between the maximum and minimum temperatures in the holder divided by the ferret diameter, for spherical, ellipsoidal, cylindrical, and cubic samples were 0.27, 0.62, 0.95 and 1.24° C/mm, respectively. From the temperature gradient perspective, the spherical and ellipsoidal shapes were the top choices.

Both rewarming rate and temperature distribution results indicated the cubic shape will not perform well the resonant chamber, which aligned with the prediction that samples with sharp edges or surfaces were inappropriate to be heated by the electromagnetic rewarming method [42].

Robinson et al. presumed that ellipsoidal sample shape works well for electromagnetic rewarming technology and performed the experiment with a cone-shape sample to approximate a ellipsoidal holder [21]. The currents from numerical modeling confirmed the fast and uniform rewarming of the ellipsoidal sample.

However, it is extremally hard to manufacture a precise ellipsoidal shape holder in the real-world. The same hardness also applied to the spherical holder. Moreover, a cryopreserved material should be stored well in an optimized holder to achieve a better rewarming performance. Thus, the material of the holder was ideally a thin-layer to diminish the absorption of the electromagnetic power. Overall, it is an engineering challenge to manufacture a qualified sample holder with desired material and dimensions in spherical or ellipsoidal geometry. Additionally, an extra supporting structure is required to hold the position of the spherical and ellipsoidal sample in the center of the cavity, which may result as the effect of the electromagnetic profile. Therefore, cylindrical holder was the best option with the fair manufacturing and faster rewarming rate. Though, more improvements should be considered to enhance the uniformity of the temperature profile.

6. Real-time resonant frequency monitoring and controlling system

Convective warming methods are hindered by the poor abilities to conduct heat into the core part of the materials. While volumetric heating method is needed for bulky material, the previous multimode or commercial microwave systems could not be adopted since they lack a precise control system to maintain the resonant state, leading to either recrystallization or devitrification. Due to the slow heating, most of electromagnetic energy was reflected back from the cavity or causing thermal runaway problems and creating undesired hot spots.

There are two major limitations for electromagnetic resonance system to achieve rapid and uniform heating. Firstly, the system itself should provide sufficient electromagnetic energy to warm up biomaterials. Secondly, the temperature dependent dielectric properties of the biomaterials progressively shift the resonant frequency of the resonant chamber during the rewarming process. Therefore, when using resonant electromagnetic field as the heating source, if the electromagnetic signal parameters remain stagnant according to the frequency change resulted from the temperature change of biomaterials, the electromagnetic energy generated may not be converted into the strong electromagnetic field in the resonant chamber to excite resonance.

Moreover, if the electromagnetic system source remains static during the rewarming procedure, severe problems regarding the system safety and efficiency may emerge. A higher portion of reflected electromagnetic power can lead to the damage to the system components as well as potential electromagnetic radiation hazards to the surrounding operators. On the other hand, with smaller electromagnetic energy remaining inside the rewarming chamber, sufficiently strong electromagnetic field inside the resonant cavity could hardly be excited resulting a slow warming. Therefore, it requires delicate control on the set up of the electromagnetic resonant system.

6.1 Electromagnetic source

The electromagnetic signal is synthesized by a signal generator (Agilent, Santa Clara, CA, USA). The signal generator can generate continuous electromagnetic waves between 250 kHz and 3 GHz which covers lower frequency band of radiofrequency and microwave. And the power output range is +7 to −120 dBm (i.e. 0.005 to 10–15 W). At this low power output, the electromagnetic field established in the resonant chamber is too weak to rewarm the cryopreserved biomaterials rapid enough avoiding devitrification. In order to intensify the electromagnetic field to achieve higher rewarming rates, a power amplifier (OPHIR RF, Los Angeles, CA, USA) was adopted to increase the electromagnetic power to over 57 dBm (501 W).

The power amplifier has a frequency range between 300 and 500 MHz, which fully covers the working frequency range for this experimental investigation. The reflected power received by this power amplifier would also be detected by the control circuits. The power amplifier will automatically cut off excessive output generation to protect itself. Due to the relatively high electromagnetic power used in the system, two side panel cooling fans were incorporated to avoid internal circuits overheating and system shutdown. The connections between the signal generator and power amplifier, as well as other microwave components are through 50 Ω coaxial cables. These cables would have some attenuation effects. Thus, in order to maintain the high power signal from the amplifier to the rest part of the system, the length should be as short as possible. The measurement was done by the signal generator and a power meter. According to the measurements of six coaxial cables of different lengths, the attenuation for coaxial cables is around 0.1 dB/m.

The most significant difference between the current resonance system and the previous assembled circuits is attributed to the frequency tracking component. During the rewarming process, the resonant frequency of the resonant cavity with biomaterials would change on account of the temperature dependent dielectric properties of the inside biological samples. To prevent the mismatch between the synthesized electromagnetic source frequency and the resonant frequency of the rewarming chamber, the generated frequency source should be dynamically adjusted during the rewarming process.

6.2 Feedback control

In order to prevent the frequency mismatch between the signal generation and the resonant frequency which is swiftly altered by the massive cryopreserved materials inside, a dynamic feedback control component was added between the electromagnetic source and the resonant cavity. A directional coupler was introduced to sample the transmitted and reflected power. A spectrum analyzer was connected to the port corresponding to the reduced reflected power. The entire spectrum of the reflected power was evaluated and by looking for the highest power peak, the frequency corresponding to the most significant reflected power was determined. During the rewarming process, the frequency generated from the electromagnetic signal source is dynamically changed corresponding to this spectrum and minimize the reflected power. Otherwise, the large portion of reflected power could lead to a slow warming rate with less power into the cavity. In addition, the reflected power can cause a serious damage to the rest part of the electromagnetic resonance system itself, such as the amplifier, signal synthesizer.

6.3 Enhancement of electric field magnitude of the resonant cavity

In the numerical simulation model, the probe length was adjusted to be the original probe length and the extended probe length. The electric field intensity excited in the sample inside the cavity was calculated. As shown in **Figure 10**, the electric field intensity in the cryopreserved material increases almost ten times larger than that using the original probe antenna, which suggests that the impedance matching between the loaded cavity and the electromagnetic source is greatly improved by adopting an extended probe antenna.

Since electric field power is proportional to the square of the electric field intensity, we could have much more power to heat the material using the optimized extended probe antenna. This numerical estimation of the electric field gives guidance to the experiment, the reflected power was measured by a network analyzer, and the quality factor of the loaded cavity was determined based on the reflection coefficient. It is

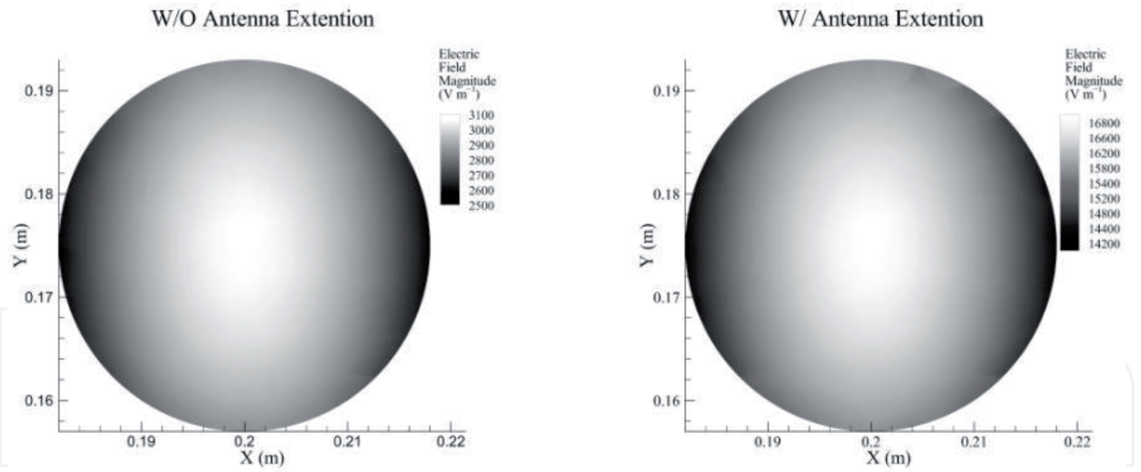

Figure 10.
Electric field intensity comparison.

found the quality factor of the loaded cavity was improved from 1681 to 5577 after adding the probe extension, which can establish a much stronger electromagnetic field inside the cavity for the rapid rewarming of the cryopreserved biomaterials.

7. Test of the electromagnetic resonance system with Jurkat cells

To experimentally evaluate the heating performance of the electromagnetic resonance system, a rewarming test of the cryopreserved Jurkat cells with large volume (25 mL) was performed. Jurkat cell is an easily accessible cell line and shares similar cryopreservation protocol to the stem cells. The testing results will guide us the future trails of cryopreservation of large system of stem cells.

7.1 Materials and methods

7.1.1 CPA solution

The CPA cocktail contains 10% (w/v) dimethyl sulfoxide (Me_2SO ; Sigma-Aldrich, St. Louis, MI, USA) and 0.25 M trehalose (Sigma-Aldrich) in culture medium (Sigma-Aldrich) solution. This CPA combination is widely used for the cryopreservation of stem cells and immune cells. The thermal and electrical properties of CPA solution were determined using methods introduced in Section 4.

7.1.2 Samples for cryopreservation

Human T lymphocyte leukemia cells (Jurkat cells) were used in the rewarming test. The Jurkat cell lines were purchased from American Type Culture Collection (Manassas, VA). Cells were cultured in the incubator that setting at 37°C, 5% carbon dioxide, and proper humidity. T25 flasks were used during the cell culture. A unit of the growth medium was prepared of 450 mL RPMI medium (life technologies), 50 mL fetal bovine serum (FBS), 5 mL Penicillin–streptomycin, and 5 mL L-glutamine.

7.1.3 Cooling process

Cylindrical sample holder contains Jurkat cell suspension was placed in a Styrofoam box, then the box was transferred to the −80°C freezer and stored there overnight. The average cooling rate was 2–3°C/min.

7.1.4 Temperature profile measurement

The temperature measurements were conducted by a fiber optic temperature meter (Neoptix Inc., Ville de Quebec, QC, Canada) during the rewarming process. The major challenge for the temperature measurement lies in the penetration through cavity wall. The cryopreserved sample remains in the center of the resonant chamber where the highest electromagnetic field was formed. However, the penetration through the cavity wall would undermine the quality factor of the resonant cavity, which means lower portion of electromagnetic energy remained inside the chamber for rewarming. Additional waveguide was designed to allow for the fiber optic temperature sensor to get through the chamber wall and maintain the quality factor at the same time. This waveguide was designed to have the cutoff frequency higher than the operating frequency during the rewarming process. Although the side effects associated with the EM waves are still in debate, it is nevertheless safer to keep away from the possible side effects caused by electromagnetic energy leakage.

At the end of the rewarming process, the surface temperature profile was recorded by an infrared temperature sensor (FLIR systems, Wilsonville, Oregon, USA). The temperature data in the central part of the cryopreserved sample recorded by the fiber optic meter and the surface temperature profile are combined to analyze the temperature gradient.

7.2 Results and discussion

7.2.1 Rewarming rate

Figure 11 shows the comparison of rewarming process of Jurkat cells between conventional water bath and electromagnetic resonance system. The average rewarming rate of water bath was 40°C/min, while increased to 90°C/min for the EM system.

7.2.2 Recovery rate of Jurkat cell

Membrane integrity was obtained by Trypan Blue (Sigma-Aldrich) staining to determine the recovery rate of Jurkat cells. **Figure 12** shows the comparison of recovery rate of Jurkat cells between conventional water bath and our

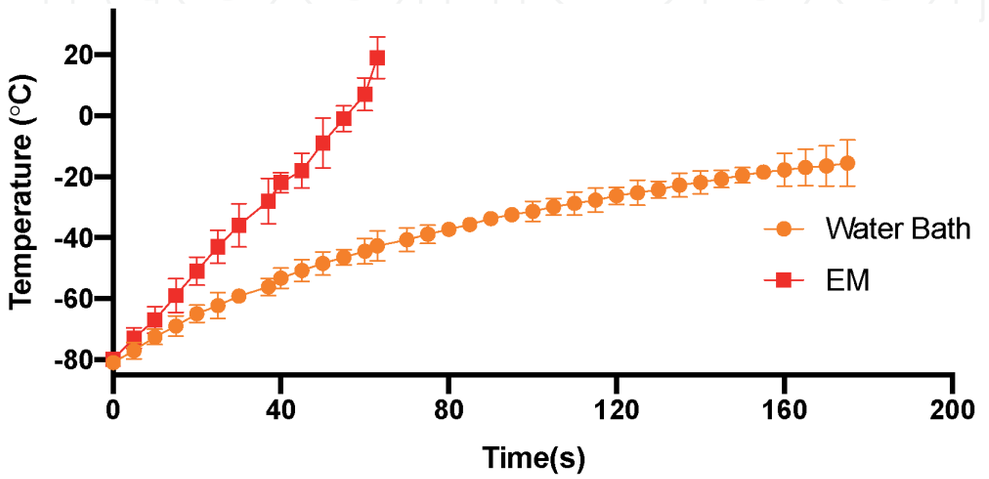

Figure 11.
Rewarming process of Jurkat cell.

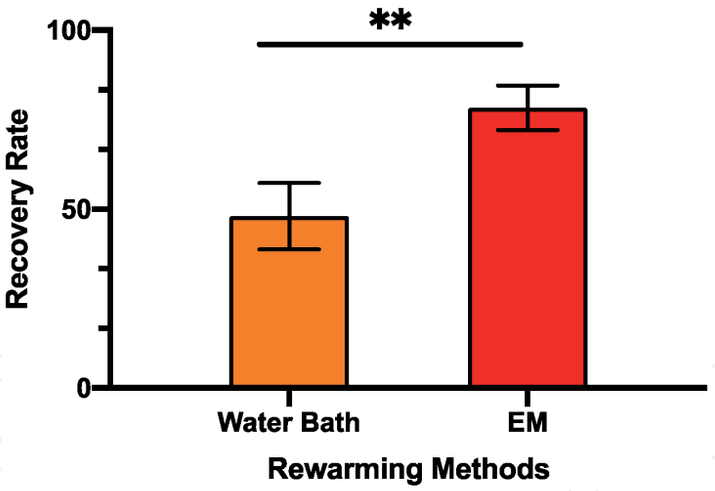

Figure 12.
Recovery rate of the Jurkat cell.

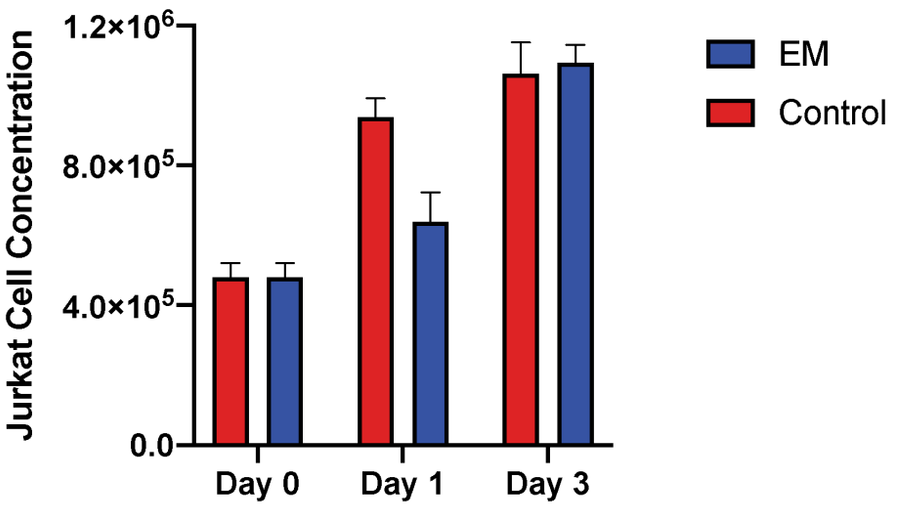

Figure 13.
Proliferation rate of the post-thawed Jurkat cell.

electromagnetic resonance system. Water bath achieved the Jurkat cell's recovery rate at $48.0 \pm 9.3\%$, while EM system significantly improved to $78.3 \pm 6.2\%$. The recovery rate obtained by EM method surpassed water bath by 63.1% ($p < 0.01$).

7.2.3 Post-thawed assessment of Jurkat cells

The post-thawed cell suspensions were cultured in a 37°C incubator with 5% carbon dioxide and proper humidity. As shown in **Figure 13**, after three days incubation, no significant change was noted to the normalized proliferation rate for the electromagnetic rewarming method. This indicates EM system does not affect Jurkat cell's cellular functionality.

8. Conclusion

In this chapter, we provide detailed information about using electromagnetic resonance system to achieve rapid-uniform rewarming in cryopreservation of stem cells. The importance of rapidly and uniformly rewarming process to the bulky system of stem cells was explained, principles of electromagnetic warming were

described, essential physical properties of CPA solution and resonance cavity were covered. Theoretical analysis and numerical simulation were introduced to improve the heating performance. A dynamic resonance frequency monitoring and control system was developed. Apart from analytical analysis, a rewarming test of Jurkat cell was performed to experimentally evaluate the electromagnetic rewarming technology. A comprehensive section on cryopreservation of large volume of stem cell has been tried to prepare, and it is aimed to provide insights about rapid-uniform rewarming during cryopreservation.

Author details

Shen Ren[1], Zhiquan Shu[1,2*], Jiaji Pan[3], Ji Peng[1], Junlan Wang[1], Chunhua Zhao[4] and Dayong Gao[1*]

1 Department of Mechanical Engineering, University of Washington, Seattle, WA, USA

2 School of Engineering and Technology, University of Washington Tacoma, Tacoma, WA, USA

3 School of Engineering and Design, Hunan Normal University, Changsha, Hunan, China

4 School of Life Sciences, Shanghai University and Institute of Basic Medical Sciences, Chinese Academy of Medical Sciences, China

*Address all correspondence to: zqshu@uw.edu and dayong@uw.edu

References

[1] Bruder, S.P., Jaiswal, N. and Haynesworth, S.E. (1997), Growth kinetics, self-renewal, and the osteogenic potential of purified human mesenchymal stem cells during extensive subcultivation and following cryopreservation. J. Cell. Biochem., 64: 278-294. doi:10.1002/(SICI)1097-4644(199702)64:2<278::AID-JCB11>3.0.CO;2-F

[2] Pegg DE. Principles of cryopreservation. Methods in molecular biology (Clifton, NJ). 2015;1257:3.

[3] Mehl PM. Nucleation and Crystal Growth in a Vitrification Solution Tested for Organ Cryopreservation by Vitrification. Cryobiology. 1993;30(5):509-518. doi:10.1006/cryo.1993.1051

[4] Mazur, P, Leibo, S.P, Chu, E.H.Y. A two-factor hypothesis of freezing injury: Evidence from Chinese hamster tissue-culture cells. Experimental Cell Research. 1972;71(2):345-355. doi:10.1016/0014-4827(72)90303-5

[5] Gao, D, Critser, J. K. Mechanisms of Cryoinjury in Living Cells. ILAR journal. 2000;41(4):187-196. doi:10.1093/ilar.41.4.187

[6] Mazur P, Mazur. Freezing of living cells: mechanisms and implications. American journal of physiology. 247(3 Pt 1):C125-C142. doi:10.1152/ajpcell.1984.247.3.C125

[7] Mazur P. Cryobiology: The Freezing of Biological Systems. Science (American Association for the Advancement of Science). 1970;168(3934):939-949. doi:10.1126/science.168.3934.939

[8] Bank H. Visualization of freezing damage. II. Structural alterations during warming. Cryobiology. 1973;10(2):157-170. doi:10.1016/0011-2240(73)90023-0

[9] Mackenzie, A.P. (2008). Death of Frozen Yeast in the Course of Slow warming. In Ciba Foundation Symposium - The Frozen Cell (eds G.E.W. Wolstenholme and M. O'Connor). doi:10.1002/9780470719732.ch6

[10] Fahy, Gregory M, Wowk, Brian, Wu, Jun. Cryopreservation of Complex Systems: The Missing Link in the Regenerative Medicine Supply Chain. Rejuvenation research. 2006;9(2):279-291. doi:10.1089/rej.2006.9.279

[11] Karlsson, Jens O.M, Toner, Mehmet. Long-term storage of tissues by cryopreservation: critical issues. Biomaterials. 1996;17(3):243-256. doi:10.1016/0142-9612(96)85562-1

[12] Brockbank KG, Chen Z, Greene ED, Campbell LH. Vitrification of heart valve tissues. Methods Mol Biol. 2015;1257:399-421. doi:10.1007/978-1-4939-2193-5_20

[13] Kuwayama M. Highly efficient vitrification for cryopreservation of human oocytes and embryos: The Cryotop method. Theriogenology. 2007;67(1):73-80. doi:10.1016/j.theriogenology.2006.09.014

[14] Ketterer, F.D, Holst, H.I, Lehr, H.B. Improved viability of kidneys with microwave thawing. Cryobiology. 1971;8(4):395-395. doi:10.1016/0011-2240(71)90197-0

[15] Guttman, Frank M, Lizin, Jacques, Robitaille, Pierre, Blanchard, Hervé, Turgeon-Knaack, Claire. Survival of canine kidneys after treatment with dimethyl-sulfoxide, freezing at −80 °C, and thawing by microwave illumination. Cryobiology. 1977;14(5):559-567. doi:10.1016/0011-2240(77)90166-3

[16] Pegg, David E, Green, Colin J, Walter, Clive A. Attempted canine renal cryopreservation using

dimethyl sulphoxide helium perfusion and microwave thawing. Cryobiology. 1978;15(6):618-626. doi:10.1016/0011-2240(78)90086-X

[17] Burdette, E.C, Karow, A.M, Jeske, A.H. Design, development, and performance of an electromagnetic illumination system for thawing cryopreserved kidneys of rabbits and dogs. Cryobiology. 1978;15(2):152-167. doi:10.1016/0011-2240(78)90020-2

[18] Ruggera, Paul S, Fahy, Gregory M. Rapid and uniform electromagnetic heating of aqueous cryoprotectant solutions from cryogenic temperatures. Cryobiology. 1990;27(5):465-478. doi:10.1016/0011-2240(90)90035-3

[19] Rachman, M.J, Evans, S, Pegg, D.E. Experimental results on the rewarming of a cryopreserved organ phantom in a UHF field. Journal of Biomedical Engineering. 1992;14(5):397-403. doi:10.1016/0141-5425(92)90085-Y

[20] Robinson, M.P, Pegg, D.E. Rapid electromagnetic warming of cells and tissues. IEEE Transactions on Biomedical Engineering. 1999;46(12):1413-1425. doi:10.1109/10.804569

[21] Robinson, Martin P, Wusteman, Monica C, Wang, Lihong, Pegg, David E. Electromagnetic re-warming of cryopreserved tissues: effect of choice of cryoprotectant and sample shape on uniformity of heating. Physics in Medicine and Biology. 2002;47(13):2311-2325. doi:10.1088/0031-9155/47/13/309

[22] Wusteman, Monica C, Pegg, David E, Robinson, Martin P, Wang, Li-Hong, Fitch, Paul. Vitrification media: toxicity, permeability, and dielectric properties. Cryobiology. 2002;44(1):24-37. doi:10.1016/S0011-2240(02)00002-0

[23] Eisenberg, David P, Taylor, Michael J, Rabin, Yoed. Thermal expansion of the cryoprotectant cocktail DP6 combined with synthetic ice modulators in presence and absence of biological tissues. Cryobiology. 2012;65(2):117-125. doi:10.1016/j.cryobiol.2012.04.011

[24] Pegg, David E, Wusteman, Monica C, Boylan, Serena. Fractures in Cryopreserved Elastic Arteries. Cryobiology. 1997;34(2):183-192. doi:10.1006/cryo.1996.1997

[25] Hasar, Ugur Cem, Oral, Emin Argun. A METRIC FUNCTION FOR FAST AND ACCURATE PERMITTIVITY DETERMINATION OF LOW-TO-HIGH-LOSS MATERIALS FROM REFLECTION MEASUREMENTS. Electromagnetic waves (Cambridge, Mass). 2010;107:397-412. doi:10.2528/PIER10071308

[26] Ansorge, Sven, Esteban, Geoffrey, Schmid, Georg. Multifrequency permittivity measurements enable on-line monitoring of changes in intracellular conductivity due to nutrient limitations during batch cultivations of CHO cells. Biotechnology Progress. 2010;26(1):272-283. doi:10.1002/btpr.347

[27] Juan-García, P, Torrents, J M. Measurement of mortar permittivity during setting using a coplanar waveguide. Measurement Science and Technology. 2010;21(4):045702. doi:10.1088/0957-0233/21/4/045702

[28] Lee, K. Y, Abbas, Z, Yeow, Y. K, Nur Sharizan, M. D, Meng, C. E. In situ measurements of complex permittivity and moisture content in oil palm fruits. European physical journal Applied physics. 2010;49(3):31201. doi:10.1051/epjap/2010007

[29] John H. Bradford, Joel T. Harper, Joel Brown. Complex dielectric permittivity measurements from ground-penetrating radar data to estimate snow liquid water content in the pendular regime. Water Resources

Research. 2009;45(8):W08403-n/a. doi:10.1029/2008WR007341

[30] Ba, Doudou, Sabouroux, Pierre. EpsiMu, A toolkit for permittivity and permeability measurement in microwave domain at real time of all materials: Applications to solid and semisolid materials. Microwave and Optical Technology Letters. 2010;52(12):2643-2648. doi:10.1002/mop.25570

[31] Zohdi, T.I, Kuypers, F.A, Lee, W.C. Estimation of red blood cell volume fraction from overall permittivity measurements. International Journal of Engineering Science. 2010;48(11):1681-1691. doi:10.1016/j.ijengsci.2010.04.013

[32] Hasar, Ugur Cem, Yurtcan, Mustafa Tolga. A microwave method based on amplitude-only reflection measurements for permittivity determination of low-loss materials. Measurement. 2010;43(9):1255-1265. doi:10.1016/j.measurement.2010.07.002

[33] Shibata K. Measurement of Complex Permittivity for Liquid Materials Using the Open-Ended Cut-Off Waveguide Reflection Method. IEICE transactions on electronics. 2010;E93-C(11):1621-1629. doi:10.1587/transele.E93.C.1621

[34] V. Komarov, Wang, S., Tang, J., Permittivity and measurements, in: K. Chang (Ed.) Encyclopedia of RF and microwave engineering (3693-3711), John Wiley and Sons, Inc, DOI: 10.1002/0471654507

[35] Mi Lin, Duane, M.H, Afsar, M.N. Cavity-Perturbation Measurement of Complex Permittivity and Permeability of Common Ferrimagnetics in Microwave-Frequency Range. IEEE Transactions on Magnetics. 2006;42(10):2885-2887. doi:10.1109/TMAG.2006.879885

[36] Waldron, R.A.: 'Perturbation theory of resonant cavities', Proceedings of the IEE - Part C: Monographs, 1960, 107, (12), p. 272-274, DOI: 10.1049/pi-c.1960.0041

[37] Robinson, M.P, Pegg, D.E. Rapid electromagnetic warming of cells and tissues. IEEE Transactions on Biomedical Engineering. 1999;46(12):1413-1425. doi:10.1109/10.804569

[38] Liang, Xin M, Sekar, Praveen K, Zhao, Gang, et al. High accuracy thermal conductivity measurement of aqueous cryoprotective agents and semi-rigid biological tissues using a microfabricated thermal sensor. Scientific reports. 2015;5(1):10377. doi:10.1038/srep10377

[39] Evans, S, Rachman, M.J, Pegg, D.E. Design of a UHF applicator for rewarming of cryopreserved biomaterials. IEEE Transactions on Biomedical Engineering. 1992;39(3):217-225. doi:10.1109/10.125006

[40] Luo, Dawei, Yu, Chun, He, Liqun, Lu, Caicheng, Gao, Dayong. Development of a single mode electromagnetic resonant cavity for rewarming of cryopreserved biomaterials. Cryobiology. 2006;53(2):288-293. doi:10.1016/j.cryobiol.2006.07.001

[41] Bai, X, Pegg, D.E, Evans, S, Penfold, J.D.J. Analysis of electromagnetic heating patterns inside a cryopreserved organ. Journal of Biomedical Engineering. 1992;14(6):459-466. doi:10.1016/0141-5425(92)90097-5

[42] Cai-Cheng Lu, Huai-Zhi Li, Dayong Gao. Combined electromagnetic and heat-conduction analysis of rapid rewarming of cryopreserved tissues. IEEE Transactions on Microwave Theory and Techniques. 2000;48(11):2185-2190. doi:10.1109/22.884213

[43] Penfold, J.D.J, Evans, S. Control of Thermal Runaway and Uniformity of Heating in the Electromagnetic Rewarming of a Cryopreserved Kidney Phantom. Cryobiology.

1993;30(5):493-508. doi:10.1006/cryo.1993.1050

[44] Han, X, Gao, D. Y, Luo, D, Yu, C, Lu, C. C. Numerical simulation of the microwave rewarming process of cryopreserved organs. Microwave and Optical Technology Letters. 2005;46(3):201-205. doi:10.1002/mop.20945

[45] Vaz, Raquel H, Pereira, José M.C, Ervilha, Ana R, Pereira, José C.F. Simulation and uncertainty quantification in high temperature microwave heating. Applied Thermal Engineering. 2014;70(1):1025-1039. doi:10.1016/j.applthermaleng.2014.06.005

[46] Basak, Tanmay, Aparna, K, Meenakshi, A, Balakrishnan, A.R. Effect of ceramic supports on microwave processing of porous food samples. International Journal of Heat and Mass Transfer. 2006;49(23):4325-4339. doi:10.1016/j.ijheatmasstransfer.2006.05.012

[47] Zhang, H, Datta, A. K, Taub, I. A, Doona, C. Electromagnetics, heat transfer, and thermokinetics in microwave sterilization. AIChE Journal. 2001;47(9):1957-1968. doi:10.1002/aic.690470907